



Adsorption of methylene blue by waste cotton activated carbon: equilibrium, kinetics, and thermodynamic studies

E. Ekrami, F. Dadashian*, M. Arami

Department of Textile Engineering, Amirkair University of Technology, 424 Hafez Ave, Tehran, Iran, Tel. +98 2164542691; email: ekrami@aut.ac.ir (E. Ekrami), Fax: +98 2166400245; email: dadashia@aut.ac.ir (F. Dadashian), Tel. +98 2164542614; email: arami@aut.ac.ir (M. Arami)

Received 18 May 2014; Accepted 26 January 2015

ABSTRACT

Waste cotton activated carbon was used as an adsorbent for the removal of methylene blue from aqueous solutions. The prepared activated carbon was characterized by pore structure analysis, Fourier transform infrared spectroscopy, and X-ray photoelectron spectroscopy. Batch adsorption studies were carried out and the effect of experimental parameters such as pH, initial dye concentration, and contact time on the adsorption was studied. The obtained equilibrium data were best fitted to the Langmuir model, with a maximum monolayer adsorption capacity of 344.82 mg/g. The kinetic data obtained at different concentrations were investigated using the pseudo-first-order, pseudo-second-order, and intraparticle diffusion models. The experimental data were found to conform to the pseudo-second-order kinetics with good correlation. The adsorption mechanism was also studied. The obtained thermodynamic parameters indicated that the adsorption process was spontaneous and endothermic in nature.

Keywords: Waste cotton fiber; Activated carbon; Adsorption; Methylene blue; Dye removal

1. Introduction

Textile dye-containing wastewater presents a serious environmental problem because most of the dyes impart toxicity and have complex aromatic molecular structures that are difficult to biodegrade when discharged into waste streams. In textile effluent, dyes can obstruct light penetration and affect photosynthetic activity of aquatic plants and raise the chemical oxygen demand of the wastewater [1–3]. Hence, the removal of dyes from textile effluents becomes one of the major environmental concerns these days.

Basic dyes are water soluble cationic dyes that are mostly used to dye anionic textile fibers such as acrylic and modacrylic fibers and, to a much lesser extent, wool, silk, modified nylons, and polyesters [4]. Most of basic dyes have high color strengths and can produce brilliant shades even at low concentrations. Methylene blue (MB) is one of the most commonly used basic dyes. It has a number of uses in different fields such as biology and chemistry, besides its application for coloration of textile fibers, leather, plastics, and paper. However, MB causes various harmful effects on human health such as eyes burning, skin irritation, nausea, vomiting, and diarrhea. If inhaled,

*Corresponding author.

the dye may cause methemoglobinemia, cyanosis, convulsions, tachycardia, and dyspnea [5,6].

A variety of processes such as adsorption, electrochemical, membrane separation, fluctuation–coagulation, oxidation, reverse osmosis, and biological treatment have been employed to remove dyes from wastewaters [2]. However, among all the methods available, adsorption is considered one of the most effective methods due to its easy availability, simplicity of design and operation, high efficiency, and ability to treat dyes in more concentrated forms [1,7].

Activated carbon is the most commonly used adsorbent, which is often characterized by its highly developed porosity and large surface area. However, high production costs make activated carbon more expensive than other adsorbents and limit its usages. In recent years, there has been a growing interest in the production of low-cost activated carbons from industrial and agricultural solid wastes [7–9].

Waste cotton fibers are generated in large quantities in different units of cotton textile mills such as cleaning, opening, carding, combing, drawing, and spinning [10,11]. On the other side, rapid development and higher production capacity of cotton textile industries resulted in higher output of waste cotton fibers. Hence, in the context of economic issues and environmental protection, there is growing interest in developing recycling processes to produce valuable products from waste cotton fibers [12,13]. Recycling of waste cotton to produce activated carbon can help to solve part of the problem of textile solid waste disposal and wastewater treatment.

The objective of the present work was to investigate the potential of the waste cotton activated carbon (WCAC) as an adsorbent in removing MB from aqueous solutions. In this way, the equilibrium, kinetic, and thermodynamic of the adsorption process were studied.

2. Materials and methods

2.1. Materials

Waste cotton fibers were collected from a textile mill, and used for preparing the activated carbon. The fibers were washed with a non-ionic surfactant (1 g/L Irgasol NA, provided by Ciba Co) for 1 h; then, rinsed with distilled water, and oven dried at 105°C for 3 h. Phosphoric acid was from Merck with 85% purity. Other chemicals also were analytical grades from Merck.

MB with a molecular weight of 319.85 (g/mol) supplied by Merck and was not purified prior to use. The structure of MB is shown in Fig. 1.

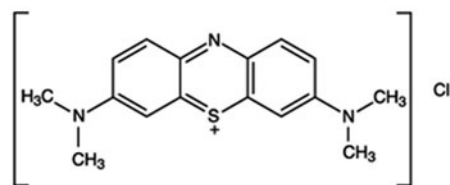


Fig. 1. Chemical structure of MB.

2.2. Preparation of activated carbon

Waste cotton fibers (20 g) were first soaked in a 300 mL solution prepared with suitable volume of 85% (w/w) aqueous H_3PO_4 and allowed to absorb the phosphoric acid overnight. The soaked waste cotton fibers were dried in an oven at 105°C, and then placed in a programmable tubular furnace (50 mm diameter and 500 mm length). Subsequently, the furnace was purged with continuous N_2 flow (50 mL/min) and heated with a controlled rate of temperature rising until activation temperature and kept at this temperature until the end of the activation process. The operational conditions were: activation temperature of 450°C, activation time of 0.5 h, impregnation ratio of 2, and the rate of temperature rising of 10°C/min. The produced AC was cooled in the furnace and washed with hot distilled water until the pH of filtrate reached to 6–7. The ratio of water to carbon was approximately 100:1 and the washing was repeated at least five times.

2.3. Characterization of activated carbon

The surface area and the pore size distribution of the activated sample were determined from nitrogen adsorption/desorption isotherms measured at 77 K by Quantachrome Autosorb equipment. The apparent surface area was derived according to the Langmuir and BET models, and the pore size distribution calculated from the desorption branch according to Barrett et al. [14].

Fourier transform infrared spectroscopy (FTIR) was performed by a Thermo Nicolet Nexus 870 spectrophotometer. For this purpose, the samples were mixed with KBr powder, compressed into discs using a manual tablet press, and analyzed using FTIR in absorbance mode.

The surface elemental contents and chemical composition of the samples were measured by X-ray photoelectron spectroscopy (XPS) using a Physical Electronics VG ESCALAB MK II XPS spectrophotometer with an achromatic MgAl X-ray source. The peak positions were adjusted based on the C_{1s} electron

binding energy (BE) corresponding to graphitic carbon, which was taken as 284.6 eV. After the baseline subtraction, deconvolution of XPS peaks was performed with a nonlinear least-square iterative technique based on the Gaussian function.

2.4. Batch equilibrium studies

Adsorption tests were carried out by adding equal mass of 0.1 g of the activated carbon in a set of 250 mL Erlenmeyer flasks containing 200 mL of MB solutions with different initial concentrations (50–600 mg/L) of the dye. The dye samples were mechanically agitated using a magnetic stirrer at 140 rpm for 240 min until the equilibrium was reached. The experiments were done at natural pH value of dye solutions which was around 6.0. At the time of $t = 0$ and equilibrium, the dye concentrations were determined by a double beam UV/vis spectrophotometer (Shimadzu, Model UV 1601, Japan) at maximum wavelength, $\lambda_{\max} = 618$ nm. The amount of adsorption at equilibrium, q_e (mg/g), was calculated by:

$$q_e = \frac{(C_0 - C_e)V}{W} \quad (1)$$

where C_0 and C_e (mg/L) are concentrations of dye at initial and equilibrium, respectively. V is the volume of the solution (L) and W is the mass of dry adsorbent used (g).

2.5. Adsorption isotherm

In order to design the adsorption process and optimize the use of adsorbents, it is important to understand the adsorption mechanisms and adsorbate–adsorbent interaction. Adsorption isotherm models relate the adsorbate concentration in the bulk to the adsorbed amount at the interface and describe how solute interacts with adsorbent. In this work, four isotherm models: the Langmuir, Freundlich, Temkin, and Dubinin–Radushkevich isotherms were examined for their ability to describe the experimental data. The validity of isotherm models to experimental data was evaluated by correlation coefficient (R^2) and normalized standard deviation, (Δq_e) % defined by Eq. (2).

$$\Delta q_e(\%) = \frac{\sqrt{\sum [(q_{e,\text{exp}} - q_{e,\text{cal}})/q_{e,\text{exp}}]^2}}{N - 1} \times 100 \quad (2)$$

where $q_{e,\text{exp}}$ (mg/g) and $q_{e,\text{cal}}$ (mg/g) are the experimental and calculated values for the amount of dyes

adsorbed, respectively. Smaller (Δq_e) represents that data from the model is similar to the experimental value, whereas larger value points out the difference between them.

2.6. Batch kinetics studies

In order to understand the dynamics of the adsorption process, the kinetic adsorption data were evaluated. The conditions of kinetic experiments were identical to those of equilibrium experiments. The samples were taken at predetermined time intervals and the MB concentration was calculated. The amount of adsorption at time t , q_t (mg/g), was measured by:

$$q_t = \frac{(C_0 - C_t)V}{W} \quad (3)$$

where C_t (mg/L) is the calculated concentration of dye at time t .

Three kinetic models, pseudo-first-order kinetic model, pseudo-second-order kinetic model, and intraparticle diffusion model were used to analyze the kinetic data. The degree of fit of kinetic models to the experimental data was evaluated by values of the correlation coefficient, R^2 and the normalized standard deviation, (Δq_t) (%) defined as:

$$\Delta q_t(\%) = \frac{\sqrt{\sum [(q_{t,\text{exp}} - q_{t,\text{cal}})/q_{t,\text{exp}}]^2}}{N - 1} \times 100 \quad (4)$$

where $q_{t,\text{exp}}$ (mg/g) and $q_{t,\text{cal}}$ (mg/g) are the experimental and calculated value for the amount of dye adsorption at time t , respectively.

3. Results and discussion

3.1. Characterization of activated carbon

Based on the Brunauer Emmett Teller analysis, the Langmuir specific surface area, BET specific surface area (S_{BET}), total micropore volume (V_{micro}), and mesopore volume (V_{meso}) of the produced activated carbon were determined as 1,101 m²/g, 694 m²/g, 0.2886 mL/g, and 0.0670 mL/g, respectively. The obtained surface area and pore volume values indicate that the produced activated carbon has well developed porous structure, in which 80.6% of the pore volume derives from the micropores. The activated carbon also contains a certain amount of mesopores that is necessary to provide transport channels for adsorbate adsorption [13].

The FTIR absorbance spectra in the range of 500–4,000 cm^{-1} for the WCAC are shown in Fig. 2. There is a strong and broad adsorption peak at 3,436 cm^{-1} , which corresponds to the stretching of the OH functional group and shows the presence of bonded hydroxide in the activated carbon sample. The produced activated carbon has peaks at 2,924 and 2,854 cm^{-1} signifying the asymmetric and symmetric CH bonds, respectively. These two peaks together with the peak at 1,458 cm^{-1} , are corresponding to the alkyl groups such as methyl and methylene groups. The C=O stretching due to carboxylic groups is observed at 1,703 cm^{-1} , while, the aromatic skeletal vibration is indicated by the band centered at 1,560 cm^{-1} . The broadband between 900 and 1,300 cm^{-1} has a maximum at 1,088.49 cm^{-1} , which may be ascribed to the P–O symmetrical vibration in a chain of P–O–P (polyphosphate) [15,16]. Generally, the absorption in this region is the characteristic of phosphorus and phosphor carbonaceous compounds.

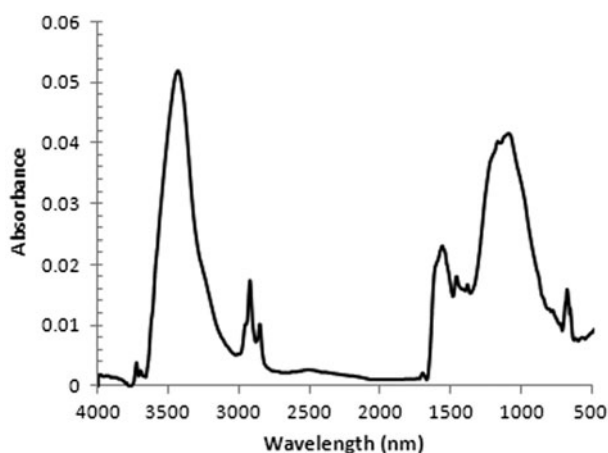


Fig. 2. The FTIR spectrum of the WCAC.

In order to further study the surface chemistry of the activated carbon, XPS technique which analyses the upper 5–10 nm of the surface of the WCAC was employed. A wide survey scan of the sample (Fig. 3(a)) shows two strong peaks for C_{1s} and O_{1s} at 284.6 and 532 eV, respectively, suggesting the presence of abundant C and O on the surface of the sample [17].

The material mainly consisted of carbon with an atomic fraction of 89% followed by oxygen with an atomic fraction of 9%. This indicates that the sample is almost carbonized. On the other hand, the presence of phosphoric acid as an activation agent caused some phosphor groups (0.6%) to get attached to the surface of activated carbon.

In order to reveal the local chemical state of functional groups on the activated carbon surface, the curve fittings of the raw data of the C_{1s} and O_{1s} spectra are presented in Fig. 3(b) and (c), respectively.

The C_{1s} spectrum was deconvoluted into three peaks with binding energies of 284.6 eV (peak 1), 286.4 eV (peak 2), and 288.6 eV (peak 3) corresponding to non-functionalized C (C–C/C–H) belonging to the carbon skeleton of graphite and to hydrocarbons, carbon in alcohol or ether groups (peak 2) and carboxyl and/or ester groups (peak 3). 61% of carbon atoms are graphitic, 16% aliphatic, and about 23% belongs to oxidized carbon.

The O_{1s} spectrum of WCAC carbon was also fitted to three peaks signifying, double bonded oxygen in C=O groups (peak 1, BE = 532.4 eV), single bonded oxygen in C–OH, C–O–C (peak 2, BE = 533.8 eV) and –COOH, chemisorbed oxygen and/or water (peak 3, BE = 535.2 eV) [18]. The obtained results from FTIR and XPS studies revealed that the bulk and surface of the activated carbon consist of various oxygen-containing functional groups. The pH of the aqueous slurry of the carbon which is mainly influenced by the

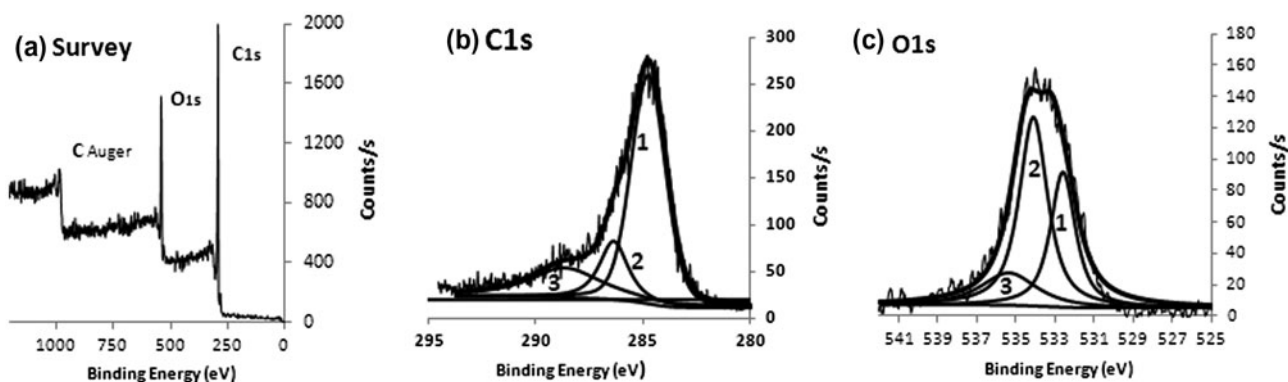


Fig. 3. XPS spectra of WCAC: (a) a wide survey scan, (b) C_{1s} spectrum, and (c) O_{1s} spectrum.

presence of oxygen or hydrogen functional groups was 4.8 and it exhibits a pH value lower than that of the blank (which was measured to be 5.5). Hence, the produced WCAC can be classified as acidic (Type L) carbons [19] which are generally preferred for the adsorption of basic compounds.

3.2. Effect of solution pH

The pH of solution is an effective parameter on both aqueous chemistry and binding sites of the adsorbent surface. Hence, the degree of adsorption of dyes onto the adsorbent surface is influenced by the solution pH. Fig. 4 shows the effect of pH on the removal of MB (initial concentration = 150 mg/L) by the WCAC. The effect of pH on adsorption of the dye was studied within pH range of 2–12. As can be seen, the percent removal of MB increased with the increase in pH and reached its maximum at pH 12. At acidic condition ($\text{pH} < \text{pH}_{\text{zpc}}$), more protons (H^+ ions) are available, which can compete with cationic dye molecules for the adsorption sites of the adsorbent and consequently decrease the amount of MB adsorption. At higher solution pH ($\text{pH} > \text{pH}_{\text{zpc}}$), the number of negatively charged sites on the adsorbent surface increases, which lead to higher adsorption of positively charged dye cations through electrostatic attraction. Similar trends of pH effect were also reported in the literature for the adsorption of basic dyes on rattan sawdust [20], activated carbons prepared from jute fiber [5], and oil palm shell [21].

3.3. Effect of initial dye concentration

In order to study the effect of initial dye concentration on the adsorption of MB by WCAC, various initial concentrations of MB solutions (50, 100, 200, 300, 400, and 600 mg/L) and time intervals were assessed

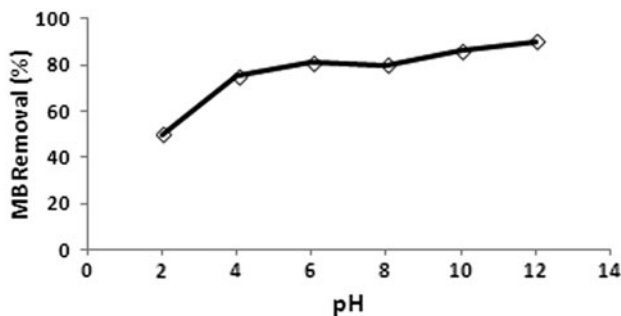


Fig. 4. Effect of solution pH on MB percent removal on WCAC (MB initial concentration = 150 mg/L).

until no adsorption of the dye on the adsorbent took place. As shown in Fig. 5, the amount of adsorbed MB per unit mass of WCAC increased from 48.85 to 346.32 mg/g as the MB concentration increased from 50 to 600 mg/L. This can be explained by an increase in the driving force of the concentration gradient, which occurs as a result of increased initial dye concentration. It was also observed that the equilibrium of adsorption was achieved faster at lower concentrations than at higher concentrations. However, for MB solutions with higher initial concentrations, the required equilibrium times were longer. The WCAC is composed of porous structure and the process of adsorption which consists of some consecutive mass transport steps is gradual and takes relatively long contact time. It is obvious that the WCAC is efficient to adsorb MB from aqueous solution and the process attaining the equilibrium is gradually especially for higher initial dye concentrations.

3.4. Adsorption isotherm

3.4.1. Langmuir isotherm

The nonlinear form of the Langmuir isotherm model [22] is represented by Eq. (5):

$$q_e = \frac{q_m C_e b}{(1 + C_e b)} \quad (5)$$

where C_e (mg/L) is the equilibrium concentration of the adsorbed MB, q_e is the amount of MB adsorbed (mg/g), q_m and b (Langmuir constants) are the monolayer adsorption capacity and affinity of adsorbent toward adsorbate, respectively. A plot of q_e against C_e

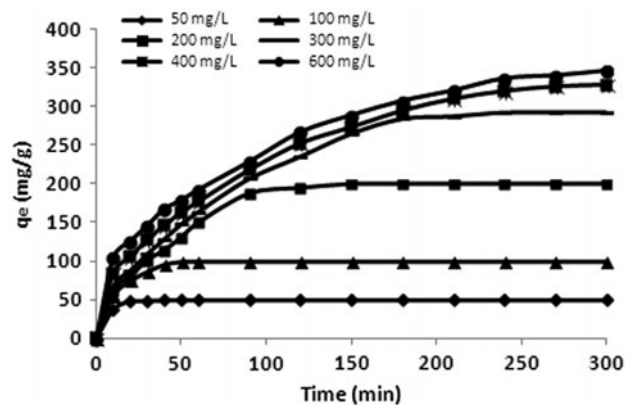


Fig. 5. Effect of initial concentration on the adsorption of MB on WCAC. Conditions: temperature = 28°C, rpm = 140, V = 200 mL, W = 0.10 g, and pH 6.

as a fitted curve is shown in Fig. 6 and the Langmuir constants were derived from the adsorption data (Table 1).

The essential characteristics of the Langmuir isotherm can be expressed by a dimensionless parameter called the separation factor (K_R) [23] which is defined as:

$$K_R = \frac{1}{(1 + K_a C_0)} \quad (6)$$

where K_R and C_0 are the Langmuir constant and the initial dye concentration (mg/L), respectively. K_R values indicate the type of isotherm to be irreversible ($K_R = 0$), favorable ($0 < K_R < 1$), linear ($K_R = 1$), or unfavorable (>1).

The obtained K_R values for the adsorption of MB on WCAC are shown in Fig. 7. The range of K_R values obtained (0.001–0.0176), indicates that the adsorption is a favorable process and that at high initial MB concentrations the adsorption is almost irreversible.

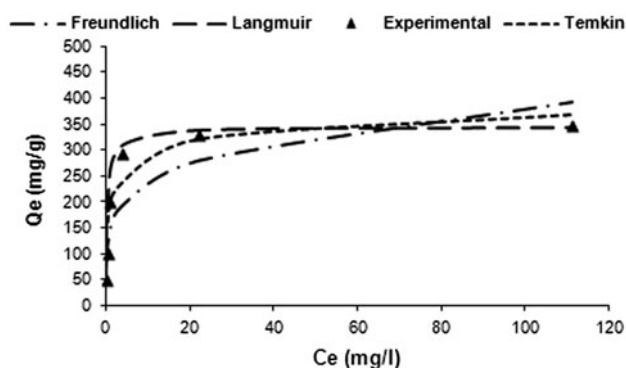


Fig. 6. The non-linear isotherms studied for adsorption of MB on WCAC. Conditions: temperature = 28°C, rpm = 140, V = 200 mL, W = 0.10 g, and pH 6.

Table 1
Langmuir, Freundlich, Temkin, and Dubinin–Radushkevich (D–R) isotherm model parameters for the adsorption of MB onto WCAC

Langmuir	q_m (mg/g)	b (L/mg)	R^2	Δq_e
	344.82	0.232	0.998	4.83
Freundlich	K_F (mg/g)	$1/n$	R^2	Δq_e
	$(L/mg)^{1/n}$	0.21	0.787	37.26
Temkin	k_T (L/mg)	B	R^2	Δq_e
	141.32	37.50	0.916	24.34
(D–R)	q_m (mg/g)	E (kJ/mol)	R^2	Δq_e
	309.92	1.118	0.980	34.56

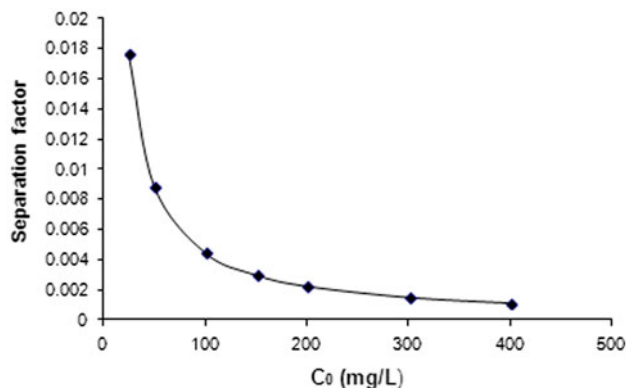


Fig. 7. The separation factor for MB adsorption on WCAC.

3.4.2. Freundlich isotherm

The nonlinear form of the Freundlich model is given [24] as:

$$q_e = K_F C_e^{1/n} \quad (7)$$

where K_F (mg/g) $(L/mg)^{1/n}$ and n are the Freundlich adsorption constants related to adsorption capacity and adsorption intensity, respectively. For the value $n = 1$, the partition between the two phases is independent of the concentration. A value of $1/n$ below one indicates a normal Langmuir isotherm, while $1/n$ above one is indicative for a cooperative adsorption [25]. A plot of q_e against C_e (Fig. 6) resulted in a poor curve fitting, which indicates that the adsorption process did not follow the model. The corresponding coefficients of the Freundlich isotherm, K_F and n are given in Table 1.

3.4.3. Temkin isotherm

In the derivation of the Temkin isotherm, it is assumed that the heat of adsorption of all molecules in the layer decrease linearly as coverage progresses [26]. The Temkin isotherm model has generally been applied in the following form:

$$q_e = RT/b_T \ln(k_T C_e) \quad (8)$$

where k_T is the equilibrium binding constant corresponding to the maximum BE and B (RT/b_T) is related to the heat of adsorption. The q_e (mg/g) and C_e (mg/L) are the experimental adsorption capacity and the concentration of the MB adsorbed at equilibrium, respectively. Also, R is the universal gas constant (8.314 J/kmol) and T is the temperature in

Kelvin (K). The graph of Temkin isotherm and the related parameters are presented in Fig. 6 and Table 1, respectively.

3.4.4. Dubinin–Radushkevich (D–R) isotherm

The D–R equation is another popular isotherm model, which its derivation is not based on ideal assumptions, such as homogeneous surface or constant adsorption potential [27]. It can give ideas about the nature of adsorption processes, whether physical or chemical. The nonlinear form of D–R model is represented as Eq. (9):

$$q_e = q_m \exp(-\beta \varepsilon^2) \quad (9)$$

where q_e and q_m are the quantity of dye molecules adsorbed on per unit weight of adsorbent (mol/g) and the maximum adsorption capacity (mol/g), respectively. ε is the Polanyi potential and can be calculated by Eq. (10):

$$\varepsilon = RT \ln \left(1 + \frac{1}{C_e} \right) \quad (10)$$

where R is the gas constant (8.314 J/mol K) and T is the absolute temperature. The constant β (mol²/J²) is the activity coefficient corresponding to adsorption mean free energy, E (kJ/mol), which can be determined by the following relationship:

$$E = \frac{1}{(2\beta)^{0.5}} \quad (11)$$

The mean free energy (E) of adsorption specifies the dominance of physical or chemical mechanism in the adsorption process. Chemical (ion-exchange) adsorption happens if the value of $E < 8$ kJ/mol, while $8 < E < 16$ kJ/mol signifies physical adsorption mechanism [26].

A plot of q_e against ε^2 gave a nonlinear graph (figure not shown) that the related obtained parameters for Dubinin–Radushkevich model are presented in Table 1.

It can be seen in Table 1 that the Langmuir model described more of the adsorption process of MB on WCAC, as the model gave the highest R^2 value (0.998) and the lowest Δq_e value (4.83%) in comparison with other three isotherm models. This indicates the homogeneous and monolayer mechanism of adsorption and the maximum monolayer adsorption capacity was 344.82 mg/g.

Although the D–R model gave relatively high R^2 values, however, the Δq_e values were higher compared to the Langmuir model.

The D–R isotherm model, the more general form of Langmuir model, further supported the physical nature of monolayer adsorption as the value of obtained mean free energy E , was less than 8 kJ/mol.

Many research works in the literature have also reported similar results where adsorption process of MB on activated carbon followed the Langmuir isotherm model, such as adsorption of MB on activated carbons produced from jute fiber [5], corncob [28], rattan sawdust [20], coconut husk [29], and oil palm fiber [21,30]. The MB adsorption capacity of the WCAC prepared in this work (344.82 mg/g) was relatively high compared to some other adsorbents reported in the literature. This indicates that waste cotton fibers are promising raw materials for the preparation of activated carbon for removal of MB from aqueous solutions.

3.5. Adsorption kinetic models

The kinetics of adsorption of MB on WCAC was investigated by applying three different kinetic models. The pseudo-first-order model proposed by Lagergren and Svenska [31] is presented by Eq. (12):

$$\ln(q_e - q_t) = \ln q_e - k_1 t \quad (12)$$

where q_e and q_t are the amount of MB adsorbed (mg/g) at equilibrium and at time t (min), respectively. k_1 is the rate constant of adsorption (min⁻¹).

The slope and intercept of the plot of $\ln(q_e - q_t)$ vs. t (figure not shown) were calculated and the model's parameters are given in Table 2.

The linear form of pseudo-second-order adsorption model [32] is expressed as Eq. (13):

$$\frac{t}{q_t} = \frac{1}{k_2 q_e^2} + \frac{1}{q_e} t \quad (13)$$

where k_2 (g/mg min) is the rate constant of pseudo-second-order adsorption.

As shown in Fig. 8, the plot of t/q_t vs. t gave very good linear relationship, and the values of q_e and k_2 were determined from the slope and the intercept of the plot. The parameters of pseudo-second-order kinetic model for the adsorption of MB on WCAC are presented in Table 2.

The R^2 values obtained from the two kinetic models were greater than 0.90 for all MB concentrations. However, the pseudo-second-order kinetic model,

Table 2

Kinetic parameters of pseudo-first and pseudo-second-order models for the adsorption of MB on WCAC

Initial MB concentration (mg/L)	$q_{e,exp}$ (mg/L)	Pseudo-first order parameters				Pseudo-second order parameters			
		$q_{e,cal}$ (mg/L)	k_1 (min^{-1})	R^2	Δq_t	$q_{e,cal}$ (mg/L)	$k_2 \times 10^3$ (min^{-1})	R^2	Δq_t
50	48.85	54.61	0.168	0.991	10.82	50.01	23.95	0.999	6.21
100	97.62	106.54	0.077	0.977	7.951	101.14	2.66	0.995	7.35
200	196.97	235.17	0.030	0.968	27.92	206.49	0.14	0.996	7.65
300	292.84	292.10	0.0186	0.962	13.85	304.25	0.041	0.996	8.66
400	328.24	369.99	0.0159	0.941	22.61	330.36	0.039	0.990	11.14
600	346.32	329.44	0.0135	0.971	21.17	339.44	0.046	0.984	13.68

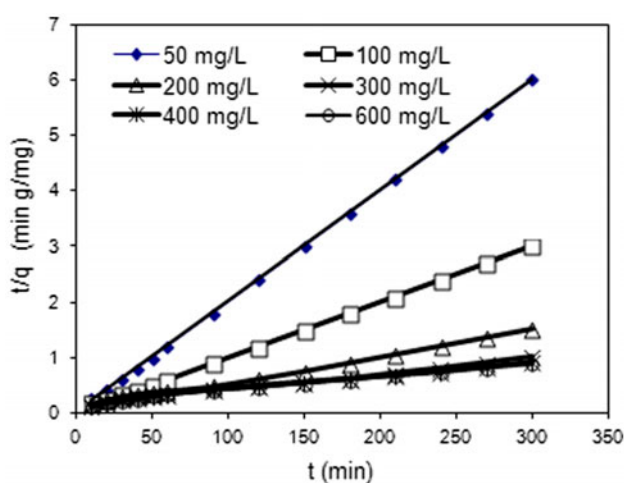


Fig. 8. Pseudo-second-order kinetic for adsorption of MB on WCAC. Conditions: temperature = 28 °C, rpm = 140, $V = 200$ mL, $W = 0.10$ g, and pH 6.

with relatively higher R^2 values (close to unity) and lower Δq_e values yielded better fit over the whole range of studied concentrations. This indicates that the pseudo-second-order kinetic model which is based on the equilibrium chemical adsorption, describes the adsorption kinetics, and that the overall rate of the dye adsorption process appears to be controlled by the chemisorption process [33].

The intraparticle diffusion model based on the theory proposed by Weber and Morris [34] was further tested to study the diffusion mechanism. The model is represented by Eq. (14):

$$q_t = k_i t^{0.5} + C \quad (14)$$

where k_i ($\text{mg/g min}^{1/2}$), the intraparticle diffusion rate constant, is obtained from the slope of the straight line of q_t vs. $t^{0.5}$ and C is the intercept.

From Eq. (14), if intra particle diffusion is the rate-limiting step, then a plot of q against $t^{0.5}$ must give a straight line with a slope that equals k_i and an intercept equal to zero. As shown in Fig. 9, the plots of q_t against $t^{0.5}$ at various initial MB concentrations are multilinear, having up to four phases of linear parts. Therefore, a piecewise linear regression method was used to fit the data to the model. The estimated intercept values for the first linear parts of all the multilinear plots are considerably different from zero. This indicates that the overall rate of adsorption is not controlled by pore diffusion at this early step and that the first linear section represents the film diffusion or chemical reaction [35]. For the next two consecutive linear segments, two pore diffusion parameters, $k_{i,1}$ and $k_{i,2}$, can be calculated from the slopes of the corresponding lines that are presented in Table 3. The rate parameters (k_i) represent the diffusion of MB in pores of distinctly different sizes such as macro pores and mesopores [36]. The decrease in pore sizes and subsequently available free path for diffusion from

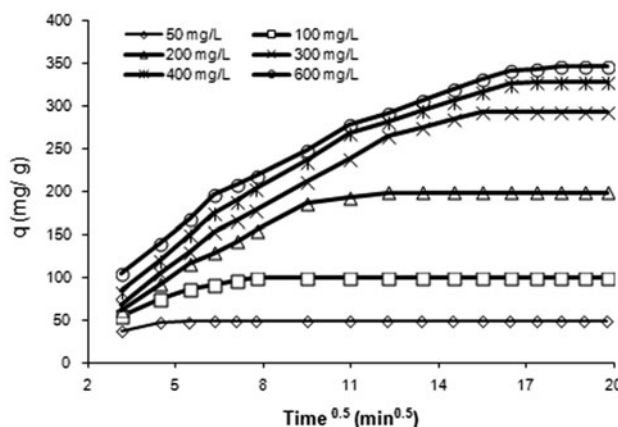


Fig. 9. Intraparticle diffusion plot for the adsorption of different initial MB concentrations. Conditions: temperature = 28 °C, rpm = 140, $V = 200$ mL, $W = 0.10$ g, and pH 6.

Table 3
Diffusion coefficients for adsorption of MB on WCAC

Initial MB concentration (mg/L)	$k_{i,1}$ (mg/g min ^{0.5})	First pore diffusion period (min)	$k_{i,2}$ (mg/g min ^{0.5})	Second pore diffusion period (min)
50	0.90	19.91–29.92	–	–
100	8.28	29.92–59.90	4.44	59.90
200	17.25	30.25–85.23	4.45	85–149.81
300	18.78	39.69–149.8	8.31	149.80–239.90
400	19.91	40.70–121.31	10.57	121.31–269.94
600	18.85	40.96–121.87	11.93	121.87–272.25

macropores to mesopores leads to a decrease in value of K_i [21]. As can be seen in Table 3, for the higher concentrations of MB, relatively higher k_i values were obtained. This can be explained by the increase of driving force for dye diffusion caused by increase in bulk liquid dye concentration. For the $C_0 = 50$ no distinct second pore diffusion period was observed. However, this does not essentially confirm that adsorption mechanism at low concentrations has no second pore-diffusion period, as the phenomenon may be occurred due to the lack of enough data points during the second period of pore diffusion.

3.6. Adsorption thermodynamic

The changes in thermodynamic parameters, standard Gibbs free energy (ΔG°), standard enthalpy (ΔH°), and standard entropy (ΔS°), for the adsorption process were studied to make a decision on whether the reaction is spontaneous or not.

The values of parameters were calculated using the Van't Hoff equation which is given as:

$$\ln K_d = \frac{-\Delta G^\circ}{RT} = \frac{\Delta S^\circ}{R} - \frac{\Delta H^\circ}{RT} \quad (15)$$

where R (8.314 J/mol K) is the universal gas constant, T (K) the absolute temperature, and K_d is the distribution coefficient which can be obtained as:

$$K_d = \frac{q_e}{C_e} \quad (16)$$

where q_e (mg/L) is the amount adsorbed on solid at equilibrium and C_e (mg/L) is the equilibrium concentration. By plotting a graph of $\ln K_d$ vs. $1/T$ the values ΔH° and ΔS° can be estimated from the slopes and intercepts. The equilibrium experiments were conducted for 200 mg/L MB solution at 30, 40, and 50 °C and the obtained thermodynamic parameters are presented in Table 4.

Table 4
Thermodynamic parameters at various temperatures studied

Standard enthalpy ΔH° (kJ/mol)	Standard entropy ΔS° (J/mol K)	Gibbs free energy ΔG° (kJ/mol)		
		323 (K)	313 (K)	303 (K)
29.45	102.61	3714.43	–2663.37	–1659.99

The negative values obtained for change of Gibbs free energy showed that the adsorption process was favorable and spontaneous and that the degree of spontaneity of the reaction increases with increasing temperature. Table 4 also indicates that the ΔS values were positive which can be occurred as a result of increased randomness or excitement at the interface (solid–liquid) during the adsorption MB on WCAC. Furthermore, the positive value of ΔH° signified that the adsorption process was endothermic in nature. Similar results were also reported for adsorption of MB on other adsorbents such as wheat shells [37], oil palm shell activated carbon [21], and acid-treated activated carbons [38].

4. Conclusions

In the present work, the applicability of WCAC to remove MB from aqueous solution was investigated. The obtained results indicate that WCAC is effective for the removal of MB from aqueous solution over a wide range of concentration. The equilibrium data for the prepared activated carbon were best represented by the Langmuir isotherm and the maximum adsorption capacity was found to be 344.82 mg/g. The adsorption kinetics followed the pseudo-second-order model with the lowest Δq_t value.

It was found that film diffusion was a rate-controlling step at the beginning of adsorption process and subsequently, diffusion in macropores and mesopores resulted in two consecutive distinct pore diffusion

stages. Investigation of thermodynamic parameters indicated that the adsorption process is spontaneous and endothermic in nature. Based on the obtained results, the WCAC could be employed as a low-cost and effective adsorbent in the removal of MB dye from wastewater.

References

- [1] M. Arami, N.Y. Limaee, N.M. Mahmoodi, N.S. Tabrizi, Removal of dyes from colored textile wastewater by orange peel adsorbent: Equilibrium and kinetic studies, *J. Colloid Interface Sci.* 288 (2005) 371–376.
- [2] C. Fernández, M.S. Larrechi, M.P. Callao, An analytical overview of processes for removing organic dyes from wastewater effluents, *TrAC Trends Anal. Chem.* 29 (2010) 1202–1211.
- [3] R. Sanghi, B. Bhattacharya, Review on decolorisation of aqueous dye solutions by low cost adsorbents, *Color. Technol.* 118 (2002) 256–269.
- [4] A.D. Broadbent, *Basic Principles of Textile Coloration*, Society of Dyers and Colourists, Thanet Press Ltd, Kent, 2001.
- [5] S. Senthilkumar, P.R. Varadarajan, K. Porkodi, C.V. Subbhuraam, Adsorption of methylene blue onto jute fiber carbon: Kinetics and equilibrium studies, *J. Colloid Interface Sci.* 284 (2005) 78–82.
- [6] V. Vadivelan, K.V. Kumar, Equilibrium, kinetics, mechanism, and process design for the sorption of methylene blue onto rice husk, *J. Colloid Interface Sci.* 286 (2005) 90–100.
- [7] S.J. Allen, B. Koumanova, Decolourisation of water/waste water using adsorption, *J. Chem. Technol. Metall.* 40 (2005) 175–192.
- [8] J.M. Dias, M.C.M. Alvim-Ferraz, M.F. Almeida, J. Rivera-Utrilla, M. Sanchez-Polo, Waste materials for activated carbon preparation and its use in aqueous-phase treatment: A review, *J. Environ. Manage.* 85 (2007) 833–846.
- [9] A. Demirbas, Agricultural based activated carbons for the removal of dyes from aqueous solutions: A review, *J. Hazard. Mater.* 167 (2009) 1–9.
- [10] M. T. Halimi, B. Azzouz, M. Ben Hassen, F. Sakli, Influence of spinning parameters and recovered fibers from cotton waste on the uniformity and hairiness of rotor spun yarn, *J. Eng. Fiber Fabr.* 4 (2009) 36–43.
- [11] Ş. Altun, Prediction of textile waste profile and recycling opportunities in turkey, *Fibers Text. East. Eur.* 20 (2012) 416–420.
- [12] T.F. Meyabadi, F. Dadashian, Optimization of enzymatic hydrolysis of waste cotton fibers for nanoparticles production using response surface methodology, *Fiber Polym.* 13 (2012) 313–321.
- [13] E. Ekrami, F. Dadashian, M. Soleimani, Waste cotton fibers based activated carbon: Optimization of process and product characterization, *Fiber Polym.* 15 (2014) 1855–1864.
- [14] E.P. Barrett, L.G. Joyner, P.P. Halenda, The determination of pore volume and area distributions in porous substances. I. Computations from nitrogen isotherms, *J. Am. Chem. Soc.* 73 (1951) 373–380.
- [15] X.U. Tao, L.I.U. Xiaoqin, Peanut shell activated carbon: Characterization, surface modification and adsorption of Pb^{2+} from aqueous solution, *Chinese, J. Chem. Eng.* 16 (2008) 401–406.
- [16] P. Patnukao, A. Kongsuwan, P. Pavasant, Batch studies of adsorption of copper and lead on activated carbon from *Eucalyptus camaldulensis* dehn. Bark, *J. Environ. Sci.* 20 (2008) 1028–1034.
- [17] S.A. Mirji, S.B. Halligudi, N. Mathew, N.E. Jacob, K.R. Patil, A.B. Gaikwad, Adsorption of methanol on mesoporous SBA, *Mater. Lett.* 61 (2006) 88–92.
- [18] A.M. Puziy, O.I. Poddubnaya, A.M. Ziatdinov, On the chemical structure of phosphorus compounds in phosphoric acid-activated carbon, *Appl. Surf. Sci.* 252 (2006) 8036–8038.
- [19] C.H. Tessmer, R. Vidic, L. Uranowski, Impact of oxygen-containing surface functional groups on activated carbon adsorption of phenols, *Environ. Sci. Technol.* 31 (1997) 1872–1878.
- [20] B.H. Hameed, M.I. El-Khaiary, Malachite green adsorption by rattan sawdust: Isotherm, kinetic and mechanism modeling, *J. Hazard. Mater.* 159 (2008) 574–579.
- [21] I.A.W. Tan, A.L. Ahmad, B.H. Hameed, Enhancement of basic dye adsorption uptake from aqueous solutions using chemically modified oil palm shell activated carbon, *Colloids Surf., A* 318 (2008) 88–96.
- [22] I. Langmuir, The constitution and fundamental properties of solids and liquids. Part I. Solids, *J. Am. Chem. Soc.* 38 (1916) 2221–2295.
- [23] K.R. Hall, L.C. Eagleton, A. Acrivos, T. Vermeulen, Pore- and solid-diffusion kinetics in fixed-bed adsorption under constant-pattern conditions, *Ind. Eng. Chem. Fundam.* 5 (1966) 212–223.
- [24] H.M.F. Freundlich, Over the adsorption in solution, *J. Phys. Chem.* 57 (1906) 385–470.
- [25] Y.X. Jiang, H.J. Xu, D.W. Liang, Z.F. Tong, Adsorption of Basic Violet 14 from aqueous solution on bentonite, *C.R. Chim.* 11 (2008) 125–129.
- [26] M.J. Temkin, V. Pyzhev, Recent modifications to Langmuir isotherms, *Acta Physicochem. USSR* 12 (1940) 217–225.
- [27] M.M. Dubinin, L.V. Radushkevich, Equation of the characteristic curve of activated charcoal, *Proc. Acad. Sci. USSR. Phys. Chem. Sect.* 55 (1947) 331–333.
- [28] R.L. Tseng, S.K. Tseng, F.C. Wu, Preparation of high surface area carbons from corncob with KOH etching plus CO_2 gasification for the adsorption of dyes and phenols from water, *Colloids Surf., A* 279 (2006) 69–78.
- [29] I.A.W. Tan, B.H. Hameed, A.L. Ahmad, Optimization of preparation conditions for activated carbons from coconut husk using response surface methodology, *Chem. Eng. J.* 137 (2008) 462–470.
- [30] I.A.W. Tan, B.H. Hameed, A.L. Ahmad, Equilibrium and kinetic studies on basic dye adsorption by oil palm fibre activated carbon, *Chem. Eng. J.* 127 (2007) 111–119.
- [31] S. Lagergren, B.K. Svenska, On the theory of so-called adsorption of dissolved substances, *R. Swed. Acad. Sci. Doc. Band* 24 (1898) 1–39.
- [32] Y.S. Ho, S. McKay, Pseudo-second order model for sorption processes, *Process Biochem.* 34 (1999) 451–465.

- [33] R.L. Tseng, S.K. Tseng, Pore structure and adsorption performance of the KOH-activated carbons prepared from corncob, *J. Colloid Interface Sci.* 287 (2005) 428–437.
- [34] W.J. Weber, J.C.S. Morris, *Proceedings of the International Conference on Water Pollution Symposium*, vol. 2. Pergamon, Oxford, 1962, pp. 231–609.
- [35] B.H. Hameed, M.I. El-Khaiary, Removal of basic dye from aqueous medium using a novel agricultural waste material: Pumpkin seed hull, *J. Hazard. Mater.* 155 (2008) 601–609.
- [36] S.J. Allen, G. McKay, K.Y.H. Khader, Intraparticle diffusion of a basic dye during adsorption onto sphagnum peat, *Environ. Pollut.* 56 (1989) 39–50.
- [37] Y. Bulut, H. Aydın, A kinetics and thermodynamics study of methylene blue adsorption on wheat shells, *Desalination* 194 (2006) 259–267.
- [38] S. Wang, Z.H. Zhu, Effects of acidic treatment of activated carbons on dye adsorption, *Dyes Pigm.* 75 (2007) 306–314.